Tests of lepton flavour universality using semitauonic B decays at LHCb

Adam Morris

Tests of lepton flavour universality using semitauonic B decays at LHCb

Adam Morris, on behalf of the LHCb collaboration

Aix Marseille Univ, CNRS/IN2P3, CPPM

10th International Workshop on the CKM Unitarity Triangle
Heidelberg, 20th September, 2018

Introduction

Lepton Flavour Universality (LFU):

- In SM, electroweak couplings of charged leptons are identical (universal).
- Difference between e, μ and τ should therefore only be driven by mass.
- Test: ratios of branching fractions to final states differing by lepton flavour.

LFU tests in semitauonic b-hadron decays:

$$R(X_c) = \frac{\mathcal{B}(X_b \to X_c \tau^+ \nu_\tau)}{\mathcal{B}(X_b \to X_c \mu^+ \nu_\mu)}.$$

(X_b: b-hadron, X_c: c-hadron)

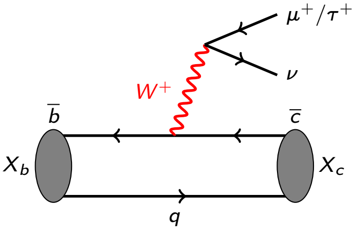

Introduction

In this talk:

- $R(D^*)$ hadronic: $B^0 \to D^{*-}\ell^+\nu$ with $\tau^+ \to 3\pi^\pm(\pi^0)\overline{\nu}_\tau$.
- $R(D^*)$ muonic: $B^0 \to D^{*-}\ell^+\nu$ with $\tau^+ \to \mu^+\nu_\mu\overline{\nu}_\tau$.
- $R(J/\psi)$ muonic: $B_c^+ \to J/\psi\,\ell^+\nu$ with $\tau^+ \to \mu^+\nu_\mu\overline{\nu}_\tau$.
- Complementary strategies: different backgrounds and systematics.
- LHCb 2011+2012 data: $3\,\mathrm{fb}^{-1}$ at $\sqrt{s} = 7\&8\,\mathrm{TeV}$.
- Using $D^{*-} \to \overline{D}^0(\to K^+\pi^-)\pi^-$ and $J/\psi \to \mu^+\mu^-$.

Mode	BF (%)
$\tau^- \to \pi^-\pi^0\nu_\tau$	25.49 ± 0.09
$\tau^- \to e^-\overline{\nu}_e\nu_\tau$	17.82 ± 0.04
$\tau^- \to \mu^-\overline{\nu}_\mu\nu_\tau$	17.39 ± 0.04
$\tau^- \to \pi^-\nu_\tau$	10.82 ± 0.05
$\tau^- \to 3\pi^\mp\nu_\tau$	9.31 ± 0.05
$\tau^- \to 3\pi^\mp\pi^0\nu_\tau$	4.62 ± 0.05

[PDG]

Predictions:

- $R(D^*) = 0.258 \pm 0.005$ [HFLAV Summer 2018]
- $R(J/\psi) \in [0.25, 0.28]$ [PLB452 (1999) 120, arXiv:0211021, PRD73 (2006) 054024, PRD74 (2006) 074008]

$R(D^*)$ with $\tau^+ \to 3\pi^\pm(\pi^0)\overline{\nu}_\tau$

$R(D^*)$ hadronic: introduction

$$\mathcal{K}(D^*) = \frac{\mathcal{B}(B^0 \to D^{*-}\tau^+\nu_\tau)}{\mathcal{B}(B^0 \to D^{*-}3\pi^\pm)} = \frac{N_{\text{sig}}}{N_{\text{norm}}}\frac{\varepsilon_{\text{norm}}}{\varepsilon_{\text{sig}}}\frac{1}{\mathcal{B}(\tau^+ \to 3\pi^\pm(\pi^0)\overline{\nu}_\tau)}$$

- Signal and normalisation same visible final state: $D^{*-}3\pi^\pm$.
- N_{sig} from 3D binned template fit:
  - $q^2 \equiv |P_{B^0} - P_{D^*}|^2$,
  - τ^+ decay time,
  - Output of BDT trained to discriminate signal from $D^*D_s^+$.
- N_{norm} from unbinned max likelihood fit to $m(D^*3\pi^\pm)$.
- Make use of three-prong tau vertex in selection.
- Convert $\mathcal{K}(D^*)$ to $R(D^*)$:

$$R(D^*) = \mathcal{K}(D^*)\frac{\mathcal{B}(B^0 \to D^{*-}3\pi^\pm)}{\mathcal{B}(B^0 \to D^{*-}\mu^+\nu_\mu)}$$

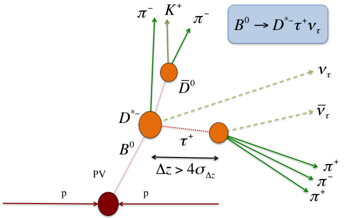

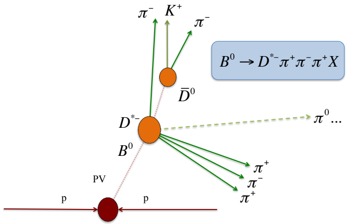

$R(D^*)$ hadronic: backgrounds

- Most abundant background: $X_b \to D^{*-}3\pi^\pm X$.
  - $\sim 100\times$ more abundant than signal.
  - Suppressed by requiring τ^+ vertex to be $4\sigma_{\Delta z}$ downstream from B vertex.
  - Improves S/B by factor 160.
- Remaining backgrounds: double charm modes with non-negligible lifetimes:
  - $X_b \to D^* D_s^+ X \sim 10\times$ signal,
  - $X_b \to D^* D^+ X \sim 1\times$ signal,
  - $X_b \to D^* D^0 X \sim 0.2\times$ signal.

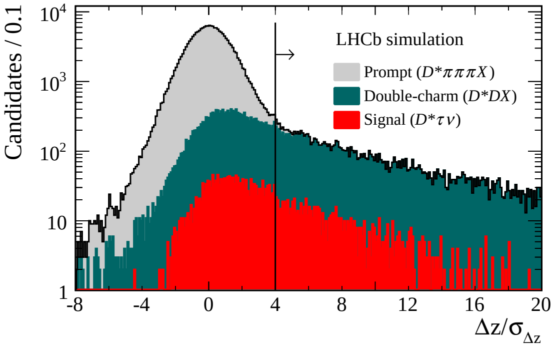

[PRD 97, 072013 (2018)]

$R(D^*)$ hadronic: backgrounds

Discriminate between signal and double charm backgrounds using a BDT that exploits the resonant structures in the $3\pi^\pm$ systems from τ^+ and D_s^+ decays.

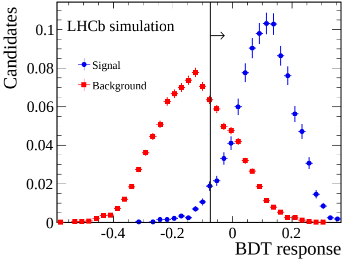

[PRD 97, 072013 (2018)]

Control samples of $D^* D_s^+ X$, $D^* D^+ X$ and $D^* D^0 X$ used to correct simulation.

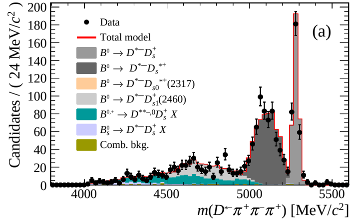

[PRL 120, 171802 (2018), PRD 97, 072013 (2018)]

$R(D^*)$ hadronic: fit and result

- Projections of 3D binned template fit shown for $t(\tau)$ (left) and q^2 (right) for each of the BDT bins.
- Signal purity increases with BDT output, while $D^* D_s^+ X$ fraction decreases.
- Dominant background at high BDT output $D^* D^+ X$ due to long D^+ lifetime.
- $N_{\text{sig}} = 1296 \pm 86,\ N_{\text{norm}} = 17660 \pm 158.$

$$\mathcal{K}(D^*) = 1.97 \pm 0.13\,(\text{stat}) \pm 0.18\,(\text{syst})$$

$$\boxed{R(D^*) = 0.291 \pm 0.019\,(\text{stat}) \pm 0.026\,(\text{syst}) \pm 0.013\,(\text{ext}).}$$

- $0.9\,\sigma$ above SM, compatible with experimental average.

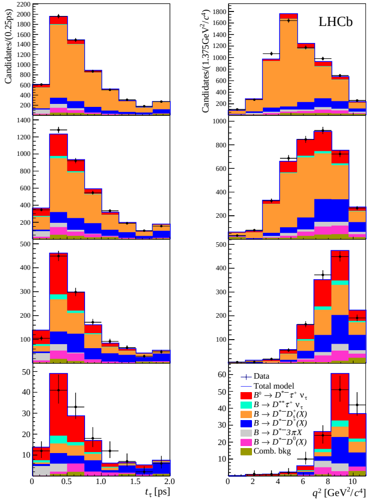

[PRL 120, 171802 (2018), PRD 97, 072013 (2018)]

$R(D^*)$ hadronic: systematic uncertainties

- Largest systematic uncertainty is MC statistics.
- Uncertainties on double charm backgrounds should improve with more data and improved external measurements.
- Uncertainty on efficiency ratio should improve with more statistics.

Source	$\frac{\delta R(D^*)}{R(D^*)}$ [%]
Simulated sample size	4.7
Empty bins in templates	1.3
Signal decay model	1.8
$D^{**}\tau\nu_\tau$ and $D_s^{**}\tau\nu_\tau$ feed-down	2.7
$D_s^+ \to 3\pi^\pm X$ decay model	2.5
$B \to D^* D_s^+ X$, $D^* D^+ X$, $D^* D^0 X$ backgrounds	3.9
Combinatorial background	0.7
$B \to D^{*-} 3\pi^\pm X$ background	2.8
Efficiency ratio	3.9
Normalisation channel efficiency (modelling of $B^0 \to D^{*-} 3\pi^\pm$)	2.0
Total systematic uncertainty	9.1

[PRL 120, 171802 (2018), PRD 97, 072013 (2018)]

$R(D^*)$ with $\tau^+ \to \mu^+ \nu_\mu \overline{\nu}_\tau$

$R(D^*)$ muonic: introduction

$$R(D^*) = \frac{\mathcal{B}(B^0 \to D^{*-}\tau^+\nu_\tau)}{\mathcal{B}(B^0 \to D^{*-}\mu^+\nu_\mu)}$$

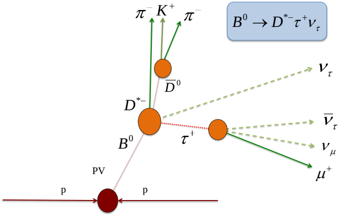

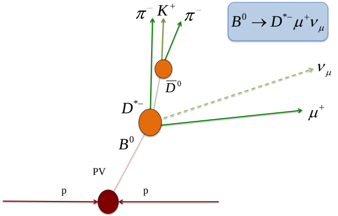

- Both modes have same visible final state: $D^{*-}\mu^+$.
- Neither fully reconstructable, due to neutrinos.
  - B^0 momentum approximated using B^0 decay vertex and scaling visible longitudinal momentum by $m(B^0)/m(D^{*-}\mu^+)$
  - Resolution on kinematic variables enough to distinguish between τ/μ modes.
- 3D binned template fit to extract yields:
  - $q^2 \equiv |P_{B^0} - P_{D^*}|^2$,
  - $m^2_{\text{miss}} \equiv |P_{B^0} - P_{D^*} - P_{\mu^+}|^2$,
  - $E^*_{\mu^+} \equiv$ muon energy in B^0 rest frame.

$R(D^*)$ muonic: fit and result

- Projections of 3D binned template fit shown for m^2_{miss} (left) and $E^*_{\mu^+}$ (right) in each of the q^2 bins
- Dominant component is $B^0 \to D^* \mu^+ \nu_\mu$
- $B^0 \to D^* \tau^+ \nu_\tau$ signal purity increases with q^2
- Backgrounds:
    - D^{**} feed-down
    - Double charm
    - Combinatorial
    - Misidentified muon

$$R(D^*) = 0.336 \pm 0.027\,(\text{stat}) \pm 0.030\,(\text{syst})$$

- $1.9\,\sigma$ above SM

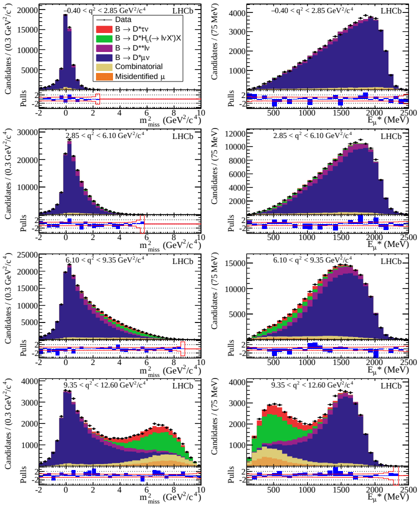

[PRL 115, 112001 (2015)]

$R(D^*)$ muonic: systematics

- MC statistics largest systematic.
- Mis-ID μ template: reduce with improved rejection and more sophisticated technique.

Source	$\delta R(D^*)[\times 10^{-2}]$
Simulated sample size (model)	2.0
Misidentified μ template shape	1.6
$\overline{B}^0 \to D^{*+}(\tau^-/\mu^-)\overline{\nu}$ form factors	0.6
$\overline{B} \to D^{*+}X_c(\to \mu\nu X')X$ shape corrections	0.5
$\mathcal{B}(\overline{B} \to D^{**}\tau^-\overline{\nu}_\tau)/\mathcal{B}(\overline{B} \to D^{**}\mu^-\nu_\mu)$	0.5
$\overline{B} \to D^{**}(\to D^*\pi\pi)\mu\nu$ shape corrections	0.4
Corrections to simulation	0.4
Combinatorial background shape	0.3
$\overline{B} \to D^{**}(\to D^{*+}\pi)\mu^-\overline{\nu}_\mu$ form factors	0.3
$\overline{B} \to D^{*+}(D_s^+ \to \tau\nu)X$ fraction	0.1
Simulated sample size (normalisation)	0.6
Hardware trigger efficiency	0.6
Particle identification efficiencies	0.3
Form-factors	0.2
$\mathcal{B}(\tau^- \to \mu^-\overline{\nu}_\mu\nu_\tau)$	< 0.1
Total systematic uncertainty	3.0

[PRL 115, 112001 (2015)]

$R(J/\psi)$ with $\tau^+ \to \mu^+ \nu_\mu \overline{\nu}_\tau$

$R(J/\psi)$ muonic: introduction

$$R(J/\psi) = \frac{\mathcal{B}(B_c^+ \to J/\psi\, \tau^+ \nu_\tau)}{\mathcal{B}(B_c^+ \to J/\psi\, \mu^+ \nu_\mu)}$$

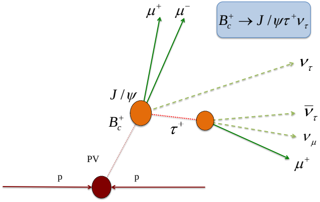

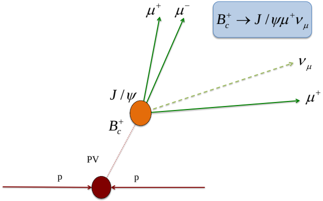

- Both modes have same visible final state: $J/\psi\, \mu^+$.
- 3D binned template fit to extract yields:
  - B_c^+ decay time,
  - m^2_{miss},
  - $Z(E^*_{\mu^+}, q^2) \equiv$ flattened 4×2 histogram of $E^*_{\mu^+}$ and q^2.
- B_c^+ decay form factors not precisely determined; constrained experimentally from this analysis.
- Low rate of B_c^+ production, but no long-lived D-meson background.

$R(J/\psi)$ muonic: fit and result

- Projections of 3D binned template fit shown.
- Largest component is $B_c^+ \to J/\psi\, \mu^+ \nu_\mu$ (19 140 $\pm$ 340 candidates).
- $B_c^+ \to J/\psi\, \tau^+ \nu_\tau$ in red (1 400 $\pm$ 300 candidates).
- Main background: $X_b \to J/\psi$ + mis-ID hadron.
- First evidence of the decay $B_c^+ \to J/\psi\, \tau^+ \nu_\tau$ ($3\,\sigma$ significance).

$$\boxed{R(J/\psi) = 0.71 \pm 0.17\,(\text{stat}) \pm 0.18\,(\text{syst})}$$

- $2\,\sigma$ above the SM.

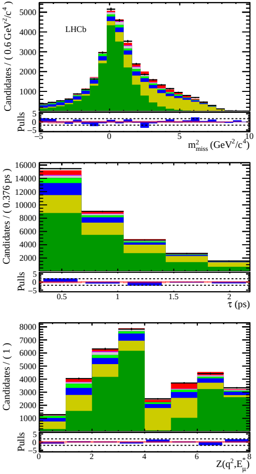

[PRL 120, 121801 (2018)]

$R(J/\psi)$ muonic: systematics

- B_c^+ form factors: recent improvements should enter into updated measurement.
- MC statistics second-largest systematic.

Source	$\delta R(J/\psi)[\times 10^{-2}]$
Simulation sample size	8.0
$B_c^+ \to J/\psi$ form factors	12.1
$B_c^+ \to \psi(2S)$ form factors	3.2
Bias correction	5.4
$B_c^+ \to J/\psi X_c X$ cocktail composition	3.6
Z binning strategy	5.6
Misidentification background strategy	5.4
Combinatorial background cocktail	4.5
Combinatorial J/ψ sideband scaling	0.9
Empirical reweighting	1.6
Semitauonic $\psi(2S)$ and χ_c feed-down	0.9
Fixing $A_2(q^2)$ slope to zero	0.3
Efficiency ratio	0.6
$\mathcal{B}(\tau^+ \to \mu^+ \nu_\mu \overline{\nu}_\tau)$	0.2
Total systematic uncertainty	17.7

[PRL 120, 121801 (2018)]

Summary and conclusions

Summary

LHCb has made 3 tests of LFU with semitauonic B decays so far:

$$
\begin{aligned}
R(D^*)\ \text{(hadronic)} &= 0.291 \pm 0.019\,(\text{stat}) \pm 0.026\,(\text{syst}) \pm 0.013\,(\text{ext}),\\
R(D^*)\ \text{(muonic)} &= 0.336 \pm 0.027\,(\text{stat}) \pm 0.030\,(\text{syst}),\\
R(J/\psi) &= 0.71 \ \ \pm 0.17 \ \ (\text{stat}) \pm 0.18 \ \ (\text{syst}).
\end{aligned}
$$

Average of LHCb $R(D^*)$ results is $1.9\,\sigma$ above SM:

$$R(D^*) = 0.310 \pm 0.016\,(\text{stat}) \pm 0.022\,(\text{syst}).$$

World averages

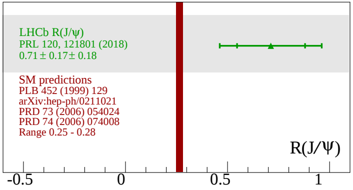

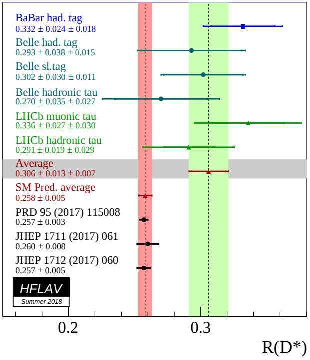

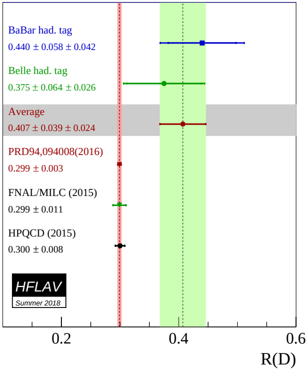

Between LHCb, BaBar and Belle: 9 measurements of LFU with semitauonic B decays so far.

- $6 \times R(D^*)$, $2 \times R(D)$, $1 \times R(J/\psi)$.
- All lie above the SM expectation.
- $R(D^*)$ average $3.0\,\sigma$ from SM.

[HFLAV Summer 2018]

$R(D)$ included for context

World averages

- HFLAV summer 2018 $R(D) - R(D^*)$ average is 3.8 σ from the SM.
- Reduction from 4.1 σ due to increase in theory uncertainties.

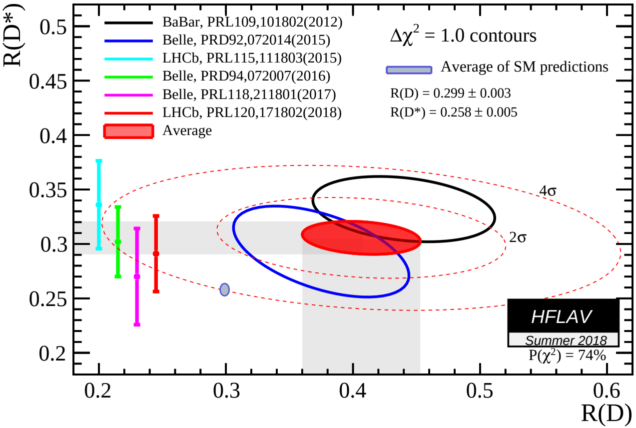

[HFLAV Summer 2018]

Conclusions and prospects

- Hints of LFU violation in semitauonic B decays.
  - $R(D) - R(D^*)$: $3.8\,\sigma$ away from SM.
  - $R(J/\psi)$: $2\,\sigma$ above SM.
- LHCb results only use Run 1 data: Runs 2,3,4... will bring much larger statistics.
- Many systematics will reduce with more data and more MC
- Others will reduce with improved external measurements (BESIII, Belle II)
- Analyses of more modes:
  - $b \to c\tau^-\overline{\nu}_\tau$: $R(D^+)$, $R(D^0)$, $R(D_s^{+(*)})$, $R(\Lambda_c^{+(*)})$ ...
  - $b \to u\tau^-\overline{\nu}_\tau$: $\Lambda_b^0 \to p\tau^-\overline{\nu}_\tau$, $B^+ \to p\overline{p}\tau^+\nu_\tau$ ...
- New observables beyond ratios of branching fractions, *e.g.* angular analyses to discriminate between NP models.

Backup slides

$R(D^*)$ with $\tau^+ \to 3\pi^\pm(\pi^0)\overline{\nu}_\tau$

$R(D^*)$ hadronic

$$R(D^*) = \mathcal{K}(D^*)\frac{\mathcal{B}(B^0 \to D^{*-}3\pi^\pm)}{\mathcal{B}(B^0 \to D^{*-}\mu^+\nu_\mu)}$$

$$\mathcal{K}(D^*) = \frac{N_{\text{sig}}}{N_{\text{norm}}}\frac{\varepsilon_{\text{norm}}}{\varepsilon_{\text{sig}}}\frac{1}{\mathcal{B}(\tau^+ \to 3\pi^\pm(\pi^0)\overline{\nu}_\tau)}$$

- N_{sig} from 3D binned template fit
- N_{norm} from unbinned fit to $m(D^{*-}3\pi^\pm)$
- Efficiencies ε from MC
- $\mathcal{B}(\tau^+ \to 3\pi^\pm\overline{\nu}_\tau) = (9.31 \pm 0.05)\,\%$ [PDG]
- $\mathcal{B}(\tau^+ \to 3\pi^\pm\pi^0\overline{\nu}_\tau) = (4.61 \pm 0.05)\,\%$ [PDG]
- $\mathcal{B}(B^0 \to D^{*-}3\pi^\pm)$ [LHCb, BaBar, Belle]
- $\mathcal{B}(B^0 \to D^{*-}\mu^+\nu_\mu)$ [PDG]

$R(D^*)$ hadronic: BDT

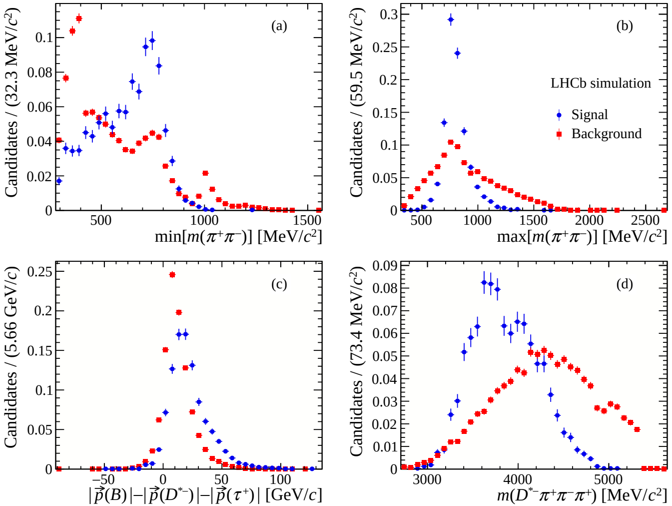

$R(D^*)$ hadronic: D_s^+, D^0, D^+ control channels

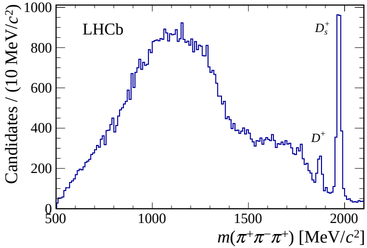

Distribution of $m(3\pi^\pm)$ for candidates passing the detached-vertex cut. The D^+ and D_s^+ peaks are visible.

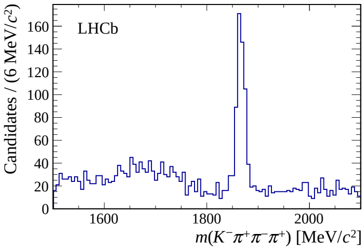

Distribution of $m(K^-3\pi^\pm)$ where a charged kaon has been associated to the $3\pi^\pm$ vertex (anti-isolation). The D^0 peak is visible.

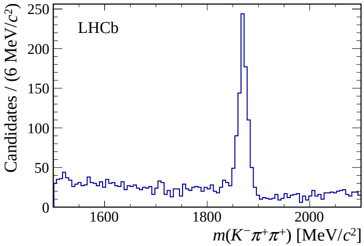

Distribution of $m(K^-\pi^+\pi^+)$ for candidates passing the signal selection, where a π^- has been assigned the kaon mass (anti-PID). The D^+ peak is visible.

$R(D^*)$ hadronic: normalisation

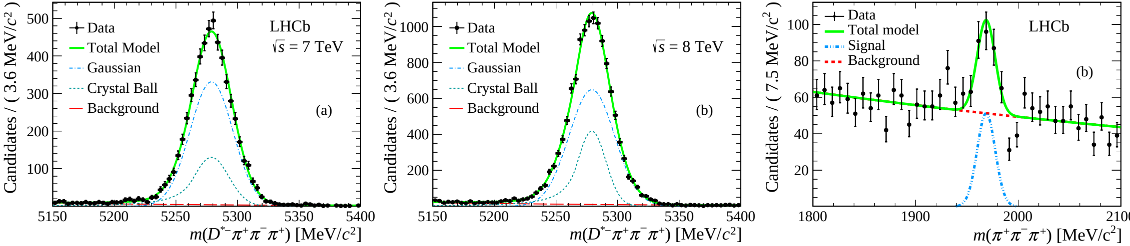

- Fit $m(D^{*-}3\pi^\pm)$ for the number of B^0 candidates
  - Signal: sum of Gaussian and Crystal Ball with shared mean
  - Background: exponential function
- Fit $m(3\pi^\pm)$ in $5.20 < m(D^{*-}3\pi^\pm) < 5.35\,\text{GeV}/c^2$ for number of D_s^+ candidates
  - Signal: Gaussian distribution
  - Background: exponential function
- N_norm is the difference of the two

$$N_\text{norm} = 17660 \pm 143\,(\text{stat}) \pm 64\,(\text{syst}) \pm 22(D_s^+)$$

$R(D^*)$ hadronic: neutral isolation

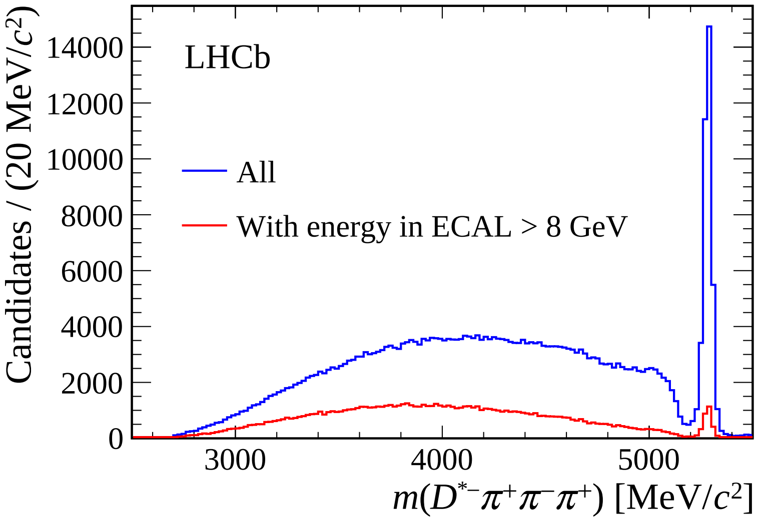

$R(D^*)$ hadronic: $X_b \to D^{*-}3\pi^\pm X$ MC sample

- Inclusive $X_b \to D^{*-}3\pi^\pm X$ MC sample
- Shown: different parents of the $3\pi^\pm$ system
  - Blue: B^0
  - Yellow: other b-hadrons
  - Signal $B^0 \to D^{*-}\tau^+\nu_\tau$
  - Prompt: directly from X_b
  - Charm (D_s^+, D^0, D^+)
  - $B1B2$: $3\pi^\pm$ and D^0 from different X_b
  - τ^+ from a D_s^+ decay
  - $D^{**}\tau^+\nu_\tau$ (*i.e.* more highly-excited $D^{(*)}$ states)
- Top: after initial selection
- Middle: all candidates in the template fit
- Bottom: 3 highest BDT bins

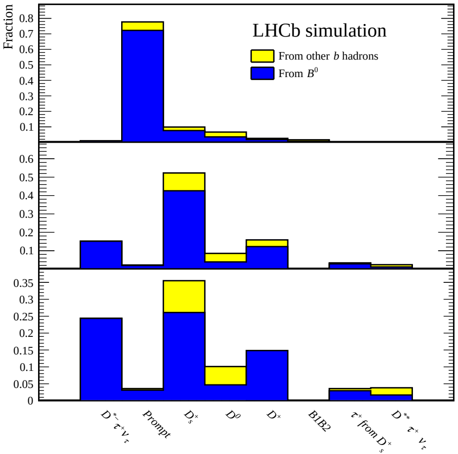

$R(D^*)$ hadronic: $D^{*-}D_s^+$ control sample

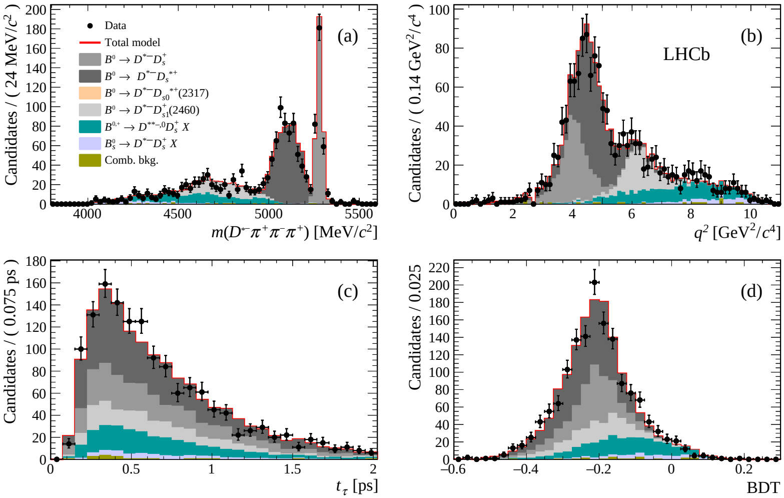

$R(D^*)$ hadronic: D_s^+ decay model

- $X_b \to D^{*-} D_s^+ X$ control sample obtained using BDT output

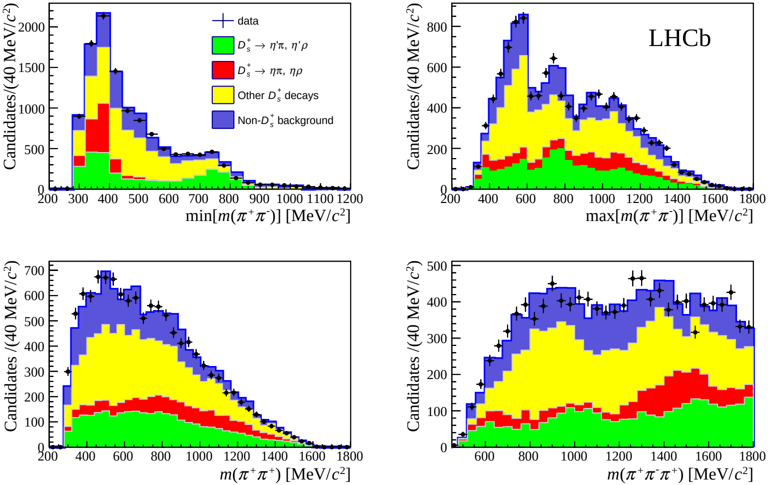

$R(D^*)$ hadronic: D_s^+ decay model

- $\tau^+ \to a_1(1260)^+(\to \rho^0\pi^+)\overline{\nu}_\tau$
- Dominant source of ρ^0 in D_s^+ decays due to $\eta' \to \rho^0\gamma$
- Crucial to describe η' contribution accurately
- Fit results used to describe the $D_s^+ \to 3\pi^\pm X$ model in the template fit

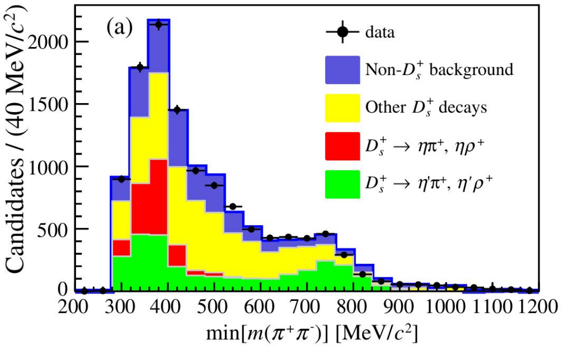

$R(D^*)$ hadronic: D_s^+ decay model fit results

D_s^+ decay	Relative contribution	Correction to MC
$\eta\pi^+(X)$	0.156 ± 0.010	
$\eta\rho^+$	0.109 ± 0.016	0.88 ± 0.13
$\eta\pi^+$	0.047 ± 0.014	0.75 ± 0.23
$\eta'\pi^+(X)$	0.317 ± 0.015	
$\eta'\rho^+$	0.179 ± 0.016	0.710 ± 0.063
$\eta'\pi^+$	0.138 ± 0.015	0.808 ± 0.088
$\phi\pi^+(X)$, $\omega\pi^+(X)$	0.206 ± 0.02	
$\phi\rho^+$, $\omega\rho^+$	0.043 ± 0.022	0.28 ± 0.14
$\phi\pi^+$, $\omega\pi^+$	0.163 ± 0.021	1.588 ± 0.208
$\eta 3\pi$	0.104 ± 0.021	1.81 ± 0.36
$\eta' 3\pi$	0.0835 ± 0.0102	5.39 ± 0.66
$\omega 3\pi$	0.0415 ± 0.0122	5.19 ± 1.53
$K^0 3\pi$	0.0204 ± 0.0139	1.0 ± 0.7
$\phi 3\pi$	0.0141	0.97
$\tau^+(\to 3\pi(N)\overline{\nu}_\tau)\nu_\tau$	0.0135	0.97
$X_{\mathrm{nr}} 3\pi$	0.038 ± 0.005	6.69 ± 0.94

$R(D^*)$ hadronic: fit projections

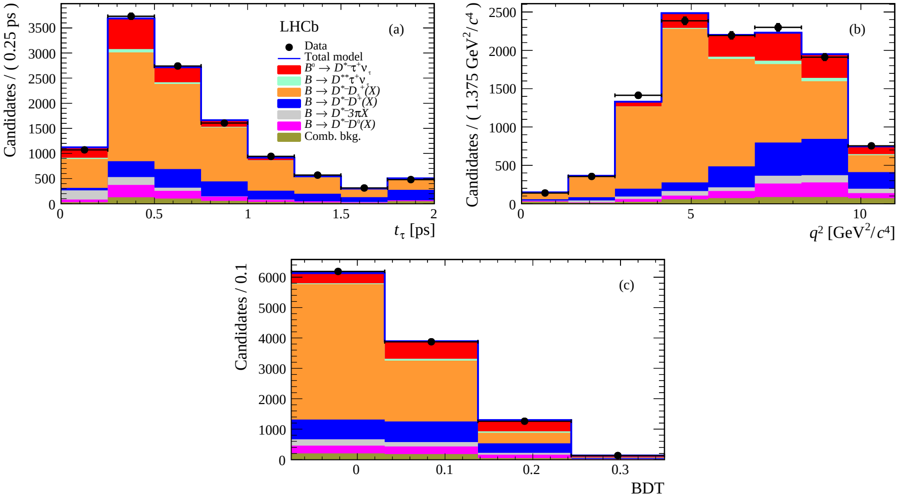

$R(D^*)$ hadronic: fit results

Fit component	Normalisation
$B^0 \to D^{*-}\tau^+(\to 3\pi\overline{\nu}_\tau)\nu_\tau$	$N_{\text{sig}} \times f_{\tau\to 3\pi\nu}$
$B^0 \to D^{*-}\tau^+(\to 3\pi\pi^0\overline{\nu}_\tau)\nu_\tau$	$N_{\text{sig}} \times (1 - f_{\tau\to 3\pi\nu})$
$B \to D^{**}\tau^+\nu_\tau$	$N_{\text{sig}} \times f_{D^{**}\tau\nu}$
$B \to D^{*-}D^+X$	$f_{D^+} \times N_{D_s}$
$B \to D^{*-}D^0X$ different vertices	$f_{D^0}^{v_1v_2} \times N_{D^0}^{\text{sv}}$
$B \to D^{*-}D^0X$ same vertex	$N_{D^0}^{\text{sv}}$
$B^0 \to D^{*-}D_s^+$	$N_{D_s} \times f_{D_s^+}/k$
$B^0 \to D^{*-}D_s^{*+}$	$N_{D_s} \times 1/k$
$B^0 \to D^{*-}D_{s0}^*(2317)^+$	$N_{D_s} \times f_{D_{s0}^{*+}}/k$
$B^0 \to D^{*-}D_{s1}(2460)^+$	$N_{D_s} \times f_{D_{s1}^+}/k$
$B^{0,+} \to D^{**}D_s^+X$	$N_{D_s} \times f_{D_s^+X}/k$
$B_s^0 \to D^{*-}D_s^+X$	$N_{D_s} \times f_{(D_s^+X)_s}/k$
$B \to D^{*-}3\pi X$	$N_{B\to D^*3\pi X}$
B1B2 combinatorics	N_{B1B2}
Combinatoric D^{*-}	$N_{\text{not}D^*}$

$R(D^*)$ hadronic: fit results

Parameter	Fit result	Constraint
N_{sig}	1296 ± 86	
$f_{\tau\to 3\pi\nu}$	0.78	0.78 (fixed)
$f_{D^{**}\tau\nu}$	0.11	0.11 (fixed)
$N_{D^0}^{\text{sv}}$	445 ± 22	445 ± 22
$f_{D^0}^{v_1 v_2}$	0.41 ± 0.22	
N_{D_s}	6835 ± 166	
f_{D^+}	0.245 ± 0.020	
$N_{B\to D^* 3\pi X}$	424 ± 21	443 ± 22
$f_{D_s^+}$	0.494 ± 0.028	0.467 ± 0.032
$f_{D_{s0}^{*+}}$	$0^{+0.010}_{-0.000}$	$0^{+0.042}_{-0.000}$
$f_{D_{s1}^+}$	0.384 ± 0.044	0.444 ± 0.064
$f_{D_s^+ X}$	0.836 ± 0.077	0.647 ± 0.107
$f_{(D_s^+ X)_s}$	0.159 ± 0.034	0.138 ± 0.040
N_{B1B2}	197	197 (fixed)
$N_{\text{not}D^*}$	243	243 (fixed)

$R(D^*)$ hadronic: more detailed systematics

Contribution	Value in %
$\mathcal{B}(\tau^+ \to 3\pi\overline{\nu}_\tau)/\mathcal{B}(\tau^+ \to 3\pi(\pi^0)\overline{\nu}_\tau)$	0.7
Form factors (template shapes)	0.7
Form factors (efficiency)	1.0
τ polarisation effects	0.4
Other τ decays	1.0
$B \to D^{**}\tau^+\nu_\tau$	2.3
$B_s^0 \to D_s^{**}\tau^+\nu_\tau$ feed-down	1.5
$D_s^+ \to 3\pi X$ decay model	2.5
D_s^+, D^0 and D^+ template shape	2.9
$B \to D^{*-}D_s^+(X)$ and $B \to D^{*-}D^0(X)$ decay model	2.6
$D^{*-}3\pi X$ from B decays	2.8
Combinatorial background (shape + normalisation)	0.7
Bias due to empty bins in templates	1.3
Size of simulation samples	4.1
Trigger acceptance	1.2
Trigger efficiency	1.0
Online selection	2.0
Offline selection	2.0
Charged-isolation algorithm	1.0
Particle identification	1.3
Normalisation channel	1.0
Signal efficiencies (size of simulation samples)	1.7
Normalisation channel efficiency (size of simulation samples)	1.6
Normalisation channel efficiency (modeling of $B^0 \to D^{*-}3\pi$)	2.0
Total uncertainty	9.1

$R(D^*)$ hadronic: feed-down systematics

- $B^0 \to D^{**}\tau\nu$ and $B^+ \to D^{**}\tau\nu$ constitute potential feed-down to the signal
- $D^{**}(2420)^0$ is reconstructed using its decay to $D^{*+}\pi^+$ **as a cross-check**
- The observation of the $D^{**}(2420)^0$ peak allows to compute the $D^{**}3\pi$ BDT distribution and to deduce a $D^{**}\tau\nu$ upper limit with the following assumption:
  - $D^{**0}\tau\nu = D^{**}(2420)^0\tau\nu$ (no sign of $D^{**}(2460)^0$)
  - $D^{**+}\tau\nu = D^{**0}\tau\nu$
- This upper limit is consistent with the theoretical prediction
- Subtraction in the signal of 0.11 ± 0.04 due to $D^{**}\tau\nu$ events leading to an error of 2.3%

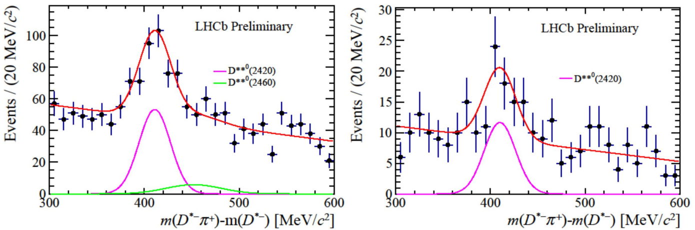

$R(D^*)$ hadronic: prospects for systematics

Source	$\frac{\delta R(D^*)}{R(D^*)}$ [%]	Future
Simulated sample size	4.7	Produce more MC (fast simulation)
Empty bins in templates	1.3	
Signal decay model	1.8	
$D^{**}\tau\nu_\tau$ and $D_s^{**}\tau\nu_\tau$ feed-down	2.7	Measure $R(D^{**}(2420)^0)$
$D_s^+ \to 3\pi^\pm X$ decay model	2.5	BESIII measurement
$B \to D^* D_s^+ X$, $D^* D^+ X$, $D^* D^0 X$ backgrounds	3.9	Improves with stats
Combinatorial background	0.7	
$B \to D^{*-} 3\pi^\pm X$ background	2.8	Stronger rejection
Efficiency ratio	3.9	Improves with stats
Normalisation channel efficiency (modelling of $B^0 \to D^{*-} 3\pi^\pm$)	2.0	
Total systematic uncertainty	9.1	

$R(D^*)$ hadronic: prospects for systematics

- Shape of $B \to D^* DX$ background (2.9%): scale with statistics
- $D_s^+ \to 3\pi X$ decay model (2.5%): BESIII future measurement.
- Branching fraction of $B^0 \to D^* 3\pi$: can be precisely measured by Belle II.
- $B \to D^{*-} 3\pi X$ background: strong cut on $\sigma_{\Delta z}$ between the τ and the D^0 vertices.
- With more data, measure $R(D^{**}(2420)^0)$ and constrain D^{**} feed-down
- Efficiency ratio: will improve with more data.

$R(D^*)$ with $\tau^+ \to \mu^+ \nu_\mu \overline{\nu}_\tau$

$R(D^*)$ muonic: kinematics

$$R(D^*) = \frac{\mathcal{B}(B^0 \to D^{*-}\tau^+\nu_\tau)}{\mathcal{B}(B^0 \to D^{*-}\mu^+\nu_\mu)}$$

with $\tau^+ \to \mu^+\nu_\mu\bar{\nu}_\tau$

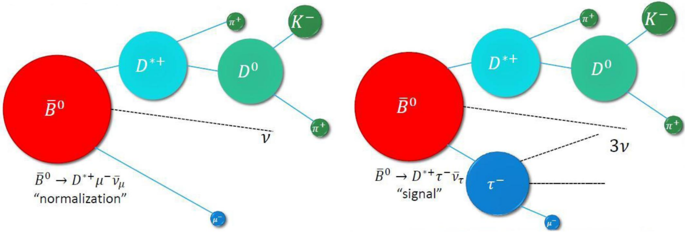

- Precise SM prediction: $R(D^*) = 0.258 \pm 0.005$ [HFLAV]
- Normalisation mode with the *same visible final state*
- $\mathcal{B}(\tau^+ \to \mu^+\nu_\mu\bar{\nu}_\tau) = (17.39 \pm 0.04)\%$
- Separate τ and μ via a $3D$ binned template fit to:
  - $q^2 \equiv |P_{B^0} - P_{D^*}|^2$,
  - $m^2_{\text{miss}} \equiv |P_{B^0} - P_{D^*} - P_{\mu^+}|^2$,
  - $E^*_{\mu^+} \equiv$ muon energy in B^0 rest frame.
- Background and signal shapes extracted from control samples and simulation validated against data

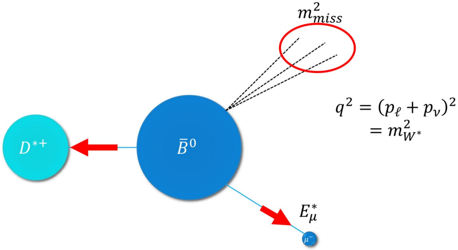

$R(D^*)$ muonic: kinematics

Problem of missing neutrino: no analytical solution for $\vec{p}_B$.
Approximate B momemtum with $p_B^z = \frac{m_B}{m_{D^*\mu}} p_{D^*\mu}^z$ and exploit the measured B flight trajectory.
This leads to $\sim$18% resolution on q^2, m^2_{miss} and E^*_μ, enough to preserve the discrimining features of the original variables.

$R(D^*)$ muonic: kinematics

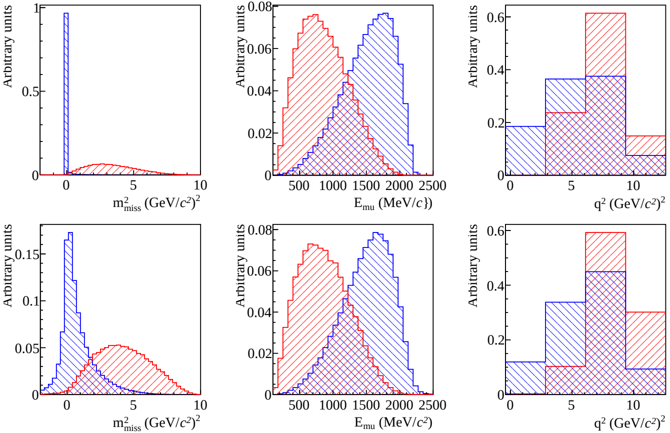

	$D^*\tau\nu_\tau$	$D^*\mu\nu_\mu$
m^2_{miss}	> 0	$\simeq 0$
E^*_μ	softer	harder
q^2	$> m^2_\tau$	> 0

τ mode (red) and μ mode (blue) using truth (top) and reconstructed (bottom) quantities.

$R(D^*)$ muonic: control samples

$\overline{B} \to [D_1, D_2^*, D_1']\mu^- \overline{\nu}_\mu$ control sample.

- Require exactly 1 track selected by the isolation MVA with the opposite charge to the D^{*+} candiadte.

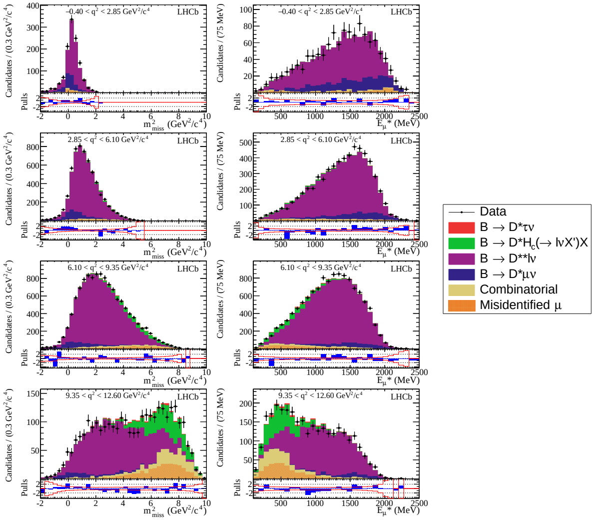

$R(D^*)$ muonic: control samples

$\overline{B} \to D^{**}(\to D^{*+}\pi^+\pi^-)\mu^-\overline{\nu}_\mu$ control sample.

- Require exactly two tracks with opposite charge selected by the isolation MVA.

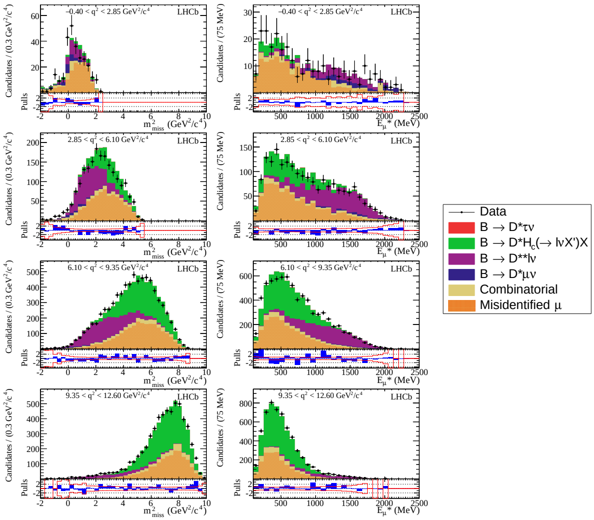

$R(D^*)$ muonic: control samples

$B \to D^{*+} X_c(\to \mu\nu X')X$ control sample.

- Require isolation MVA to identify a track consistent with the B vertex and at least one track with $K^{\pm}$ hypothesis near the B.

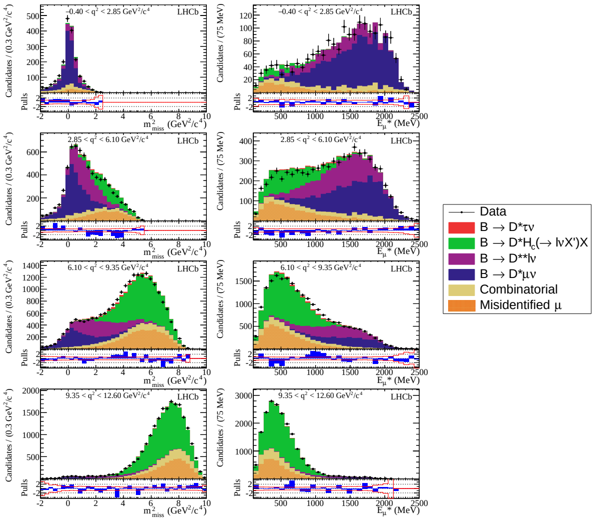

$R(D^*)$ muonic: fit projections

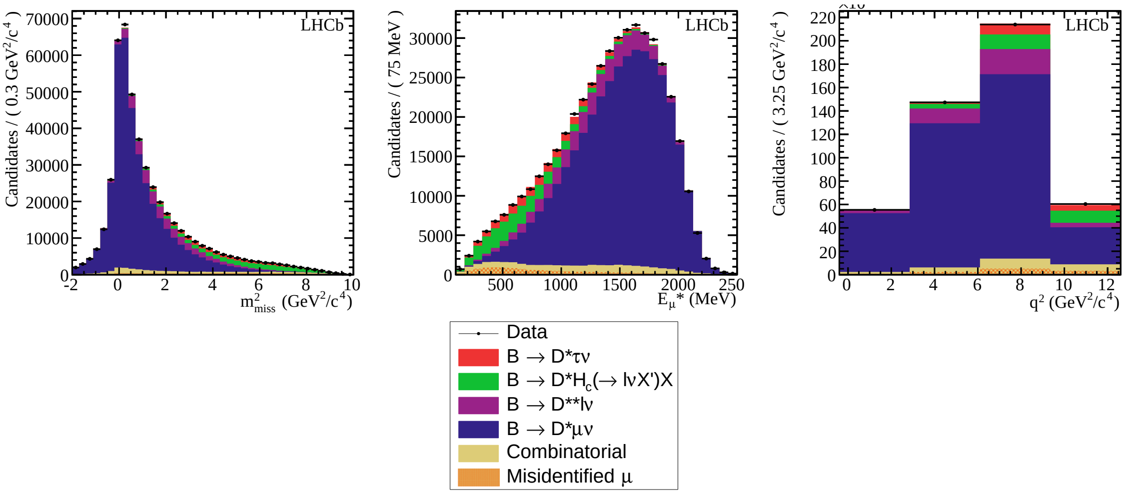

$R(J/\psi)$ with $\tau^+ \to \mu^+ \nu_\mu \overline{\nu}_\tau$

$R(J/\psi)$ muonic

- Generalisation of $R(D^*)$ to B_c^+

$$R(J/\psi) = \frac{\mathcal{B}(B_c^+ \to J/\psi\, \tau^+ \nu_\tau)}{\mathcal{B}(B_c^+ \to J/\psi\, \mu^+ \nu_\mu)}$$

- Prediction: $R(J/\psi) \in [0.25, 0.28]$ [PLB452 (1999) 120, arXiv:0211021, PRD73 (2006) 054024, PRD74 (2006) 074008]
- B_c^+ decay form factors not yet precise
- Like in $R(D^*)$, use m^2_{miss}, E^*_μ and q^2. Add information from B_c^+ decay time
- Imperfect reconstruction due to missing neutrinos. The broad shapes of the distributions are smeared but their discriminating power is preserved

$R(J/\psi)$ muonic: kinematics

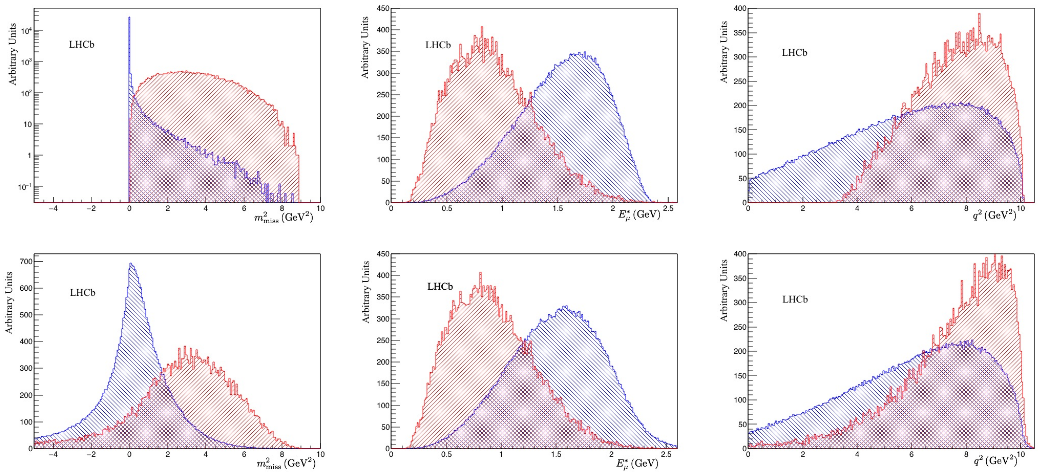

τ mode (red) and μ mode (blue) using truth (top) and reconstructed (bottom) quantities.

$R(J/\psi)$ muonic: Z variable

Trick to make a 3D fit with 4 variables: the Z variable merges information from q^2 and E^*_μ

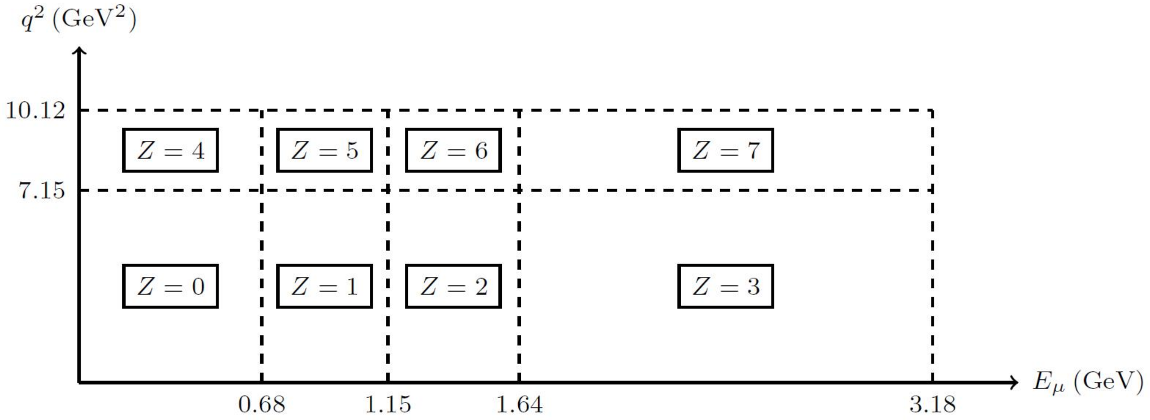

$R(J/\psi)$ muonic: fit projections in bins of Z

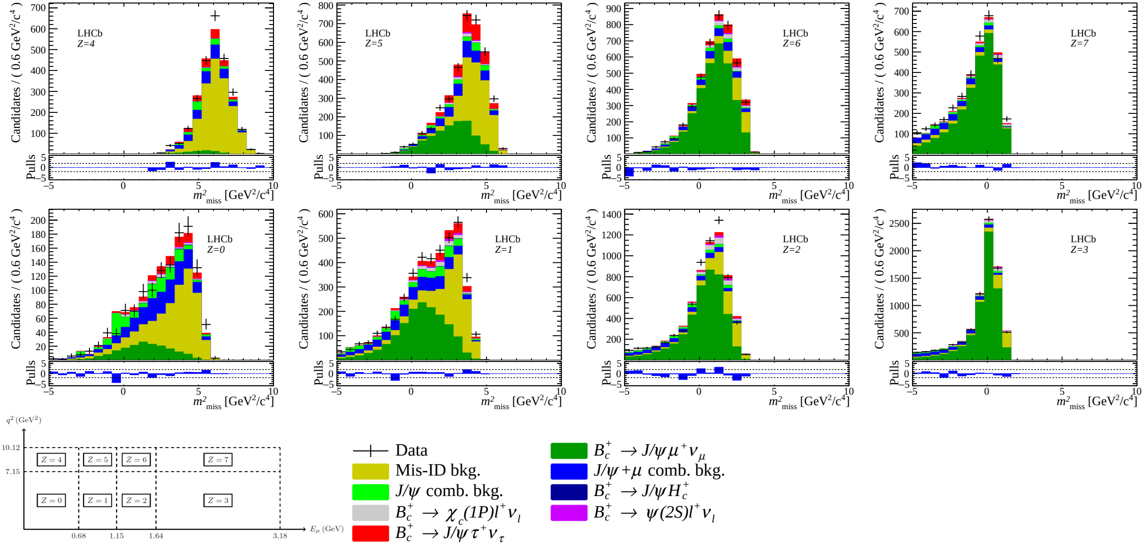

$R(J/\psi)$ muonic: fit projections in bins of Z

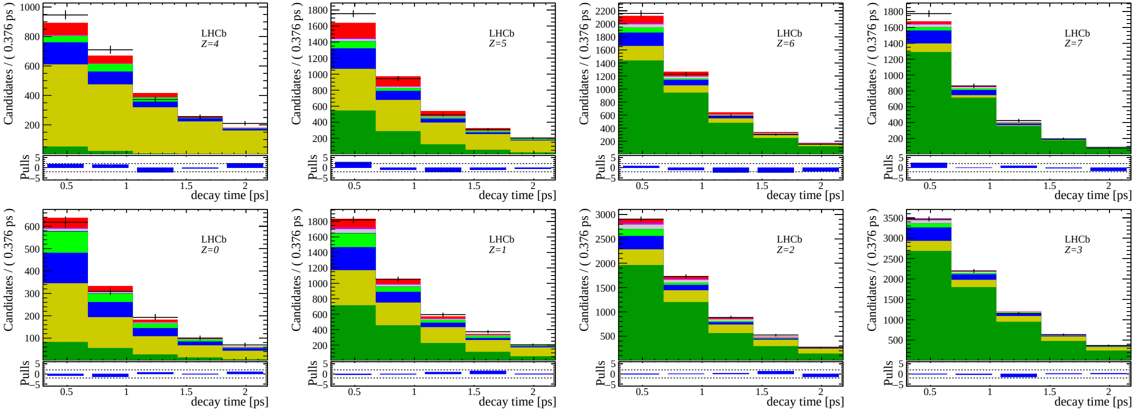

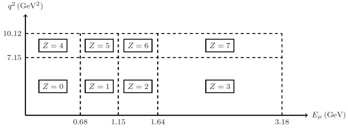

Data
Mis-ID bkg.
J/ψ comb. bkg.
$B_c^+ \to \chi_c(1P) l^+ \nu_l$
$B_c^+ \to J/\psi \tau^+ \nu_\tau$
$B_c^+ \to J/\psi \mu^+ \nu_\mu$
$J/\psi + \mu$ comb. bkg.
$B_c^+ \to J/\psi H_c^+$
$B_c^+ \to \psi(2S) l^+ \nu_l$

$R(J/\psi)$ muonic: feed-down

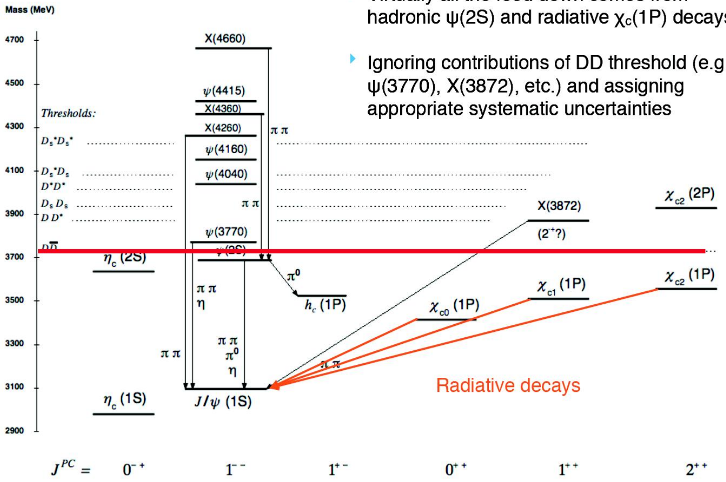

- Virtually all the feed down comes from hadronic ψ(2S) and radiative χ_c(1P) decays
- Ignoring contributions of DD threshold (e.g. ψ(3770), X(3872), etc.) and assigning appropriate systematic uncertainties

Angular observables

Full angular distribution in $B \to D^*(\to D\pi)\ell\overline{\nu}_\ell$

The full angular distribution is given by

$$\frac{d^4\Gamma}{dq^2 d\cos\theta_\ell d\cos\theta_D d\chi} = \frac{3G_F^2|V_{cb}|^2}{256(2\pi)^4 m_B^3} q^2 \left(1-\frac{m_\ell^2}{q^2}\right)^2 \sqrt{\lambda_{D^*}(q^2)} \times B(D^* \to D\pi) \times \Bigg\{$$

$$[|H_+|^2 + |H_-|^2]\left(1+\cos^2\theta_\ell + \frac{m_\ell^2}{q^2}\sin^2\theta_\ell\right)\sin^2\theta_D + 2[|H_+|^2 - |H_-|^2]\cos\theta_\ell\sin^2\theta_D$$

$$+ 4|H_0|^2\left(\sin^2\theta_\ell + \frac{m_\ell^2}{q^2}\cos^2\theta_\ell\right)\cos^2\theta_D + 4|H_t|^2\frac{m_\ell^2}{q^2}\cos^2\theta_D$$

$$- 2\beta_\ell^2\left(\Re[H_+H_-^*]\cos 2\chi + \Im[H_+H_-^*]\sin 2\chi\right)\sin^2\theta_\ell\sin^2\theta_D$$

$$- \beta_\ell^2\left(\Re[H_+H_0^* + H_-H_0^*]\cos\chi + \Im[H_+H_0^* - H_-H_0^*]\sin\chi\right)\sin 2\theta_\ell\sin 2\theta_D$$

$$- 2\Re\left[H_+H_0^* - H_-H_0^* - \frac{m_\ell^2}{q^2}(H_+H_t^* + H_-H_t^*)\right]\cos\chi\sin\theta_\ell\sin 2\theta_D$$

$$- 2\Im\left[H_+H_0^* + H_-H_0^* - \frac{m_\ell^2}{q^2}(H_+H_t^* - H_-H_t^*)\right]\sin\chi\sin\theta_\ell\sin 2\theta_D + 8\Re[H_0H_t^*]\frac{m_\ell^2}{q^2}\cos\theta_\ell\cos^2\theta_D\Bigg\}$$

$$\beta_\ell(q^2) = \sqrt{1-\frac{m_\ell^2}{q^2}}$$

$$H(q^2) = \widetilde{\varepsilon}^{\mu *}\langle D^*(\varepsilon)|J_\mu|\overline{B}\rangle$$

$B \to D^*(\to D\pi)\ell\overline{\nu}_\ell$: observables sensitive to NP

What can be extracted from the proposed observables:

$d\Gamma/dq^2$	$\left[\lvert H_+\rvert^2 + \lvert H_-\rvert^2 + \lvert H_0\rvert^2\right]\left(1+\frac{m_\ell^2}{2q^2}\right) + \frac{3}{2}\frac{m_\ell^2}{q^2}\lvert H_t\rvert^2$	
$1-\mathcal{A}_{\lambda_\ell}$	$\lvert H_+\rvert^2 + \lvert H_-\rvert^2 + \lvert H_0\rvert^2 + 3\lvert H_t\rvert^2$	
$\mathcal{A}_{\mathrm{FB}}$	$\lvert H_+\rvert^2 - \lvert H_-\rvert^2 + 2\frac{m_\ell^2}{q^2}\Re\left[H_0 H_t^*\right]$	
$R_{L,T}$	$\lvert H_+\rvert^2 + \lvert H_-\rvert^2$	
A_5	$\lvert H_+\rvert^2 - \lvert H_-\rvert^2$	
C_χ	$\Re\left[H_+ H_-^*\right]$	
S_χ	$\Im\left[H_+ H_-^*\right]$	(=0 in the SM)
A_8	$\Im\left[(H_+ + H_-)H_0^* - \frac{m_\ell^2}{q^2}\left(H_+ - H_-\right)H_t^*\right]$	(=0 in the SM)
A_9	$\Re\left[(H_+ - H_-)H_0^* - \frac{m_\ell^2}{q^2}\left(H_+ + H_-\right)H_t^*\right]$	
A_{10}	$\Im\left[(H_+ - H_-)H_0^*\right]$	(=0 in the SM)
A_{11}	$\Re\left[(H_+ + H_-)H_0^*\right]$	

Best discriminating variable to NP

$$
\begin{aligned}
Heff = \frac{G_F}{\sqrt{2}} V_{cb} \Big[& (1 + \boxed{g_V})\bar{c}\gamma_\mu b \\
& + (-1 + \boxed{g_A})\bar{c}\gamma_\mu\gamma_5 b \\
& + \boxed{g_S}\, i\partial_\mu(\bar{c}b) \\
& + \boxed{g_P}\, i\partial_\mu(\bar{c}\gamma_5 b) \\
& + \boxed{g_T}\, i\partial_\nu(\bar{c}i\sigma_{\mu\nu}b) \Big] (\bar{\ell}\gamma^\mu(1-\gamma_5)\nu_\ell)
\end{aligned}
$$

$\times$: "not sensitive"

$\star\star\star$: "maximally sensitive"

Quantity	g_V	g_A	g_S	g_P	g_T
$\mathcal{A}_{FB}^{D}$	$\times$	$-$	$\star\star\star$	$-$	$\star$
$\mathcal{A}_{\lambda_\tau}^{D}$	$\times$	$-$	$\star\star\star$	$-$	$\star\star$
$\mathcal{A}_{FB}^{D^*}$	$\star$	$\star\star\star$	$-$	$\star\star\star$	$\star$
$\mathcal{A}_{\lambda_\tau}^{D^*}$	$\times$	$\times$	$-$	$\star\star$	$\star$
$R_{L,T}$	$\times$	$\times$	$-$	$\star\star$	$\star\star$
A_5	$\star\star$	$\star\star$	$-$	$\star$	$\star\star\star$
C_χ	$\star$	$\times$	$-$	$\star\star$	$\star\star$
S_χ	$\star\star\star$	$\star\star\star$	$-$	$\times$	$\star\star\star$
A_8	$\star\star$	$\star\star$	$-$	$\star\star$	$\star\star\star$
A_9	$\star$	$\star$	$-$	$\star\star$	$\star\star$
A_{10}	$\star\star$	$\star\star$	$-$	$\times$	$\star\star$
A_{11}	$\times$	$\times$	$-$	$\star\star$	$\star\star$